The effect of boron implant energy on transient enhanced diffusion in silicon

J. Liu and V. Krishnamoorthy
Department of Materials Science and Engineering, University of Florida, Gainsville, Florida 32611

H.-J. Gossman
Lucent Technologies, Murray Hill, New Jersey 07974

L. Rubin
Eaton Corporation, Semiconductor Equipment Division, 108 Cherry Hill Drive, Beverly, Massachusetts 01915

M. E. Law
Department of Electrical Engineering, University of Florida, Gainsville, Florida 32611

K. S. Jones[a)]
Department of Materials Science and Engineering, University of Florida, Gainsville, Florida 32611

(Received 30 September 1996; accepted for publication 5 November 1996)

Transient enhanced diffusion (TED) of boron in silica after low energy boron implantation and annealing was investigated using boron-doping superlattices (DSLs) grown by low temperature molecular beam epitaxy. Boron ions were implanted at 5, 10, 20, and 40 keV at a constant dose of $2\times10^{14}/cm^2$. Subsequent annealing was performed at 750 °C for times of 3 min, 15 min, and 2 h in a nitrogen ambient. The broadening of the boron spikes was measured by secondary ion mass spectroscopy and simulated. Boron diffusivity enhancement was quantified as a function of implant energy. Transmission electron microscopy results show that ⟨311⟩ defects are only seen for implant energies ⩾10 keV at this dose and that the density increases with energy. DSL studies indicate the point defect concentration in the background decays much slower when ⟨311⟩ defects are present. These results imply there are at least two sources of TED for boron implants (B-I): short time component that decays rapidly consistent with nonvisible B-I pairs and a longer time component consistent with interstitial release from the ⟨311⟩ defects. © *1997 American Institute of Physics*. [S0021-8979(97)01104-3]

I. INTRODUCTION

Device miniaturization demands the fabrication of shallow (<1000 Å) p/n junctions.[1] There is much interest in using only low energy B+ implants to form $p+$ junctions as opposed to the present use of either BF_2^+ implants or preamorphization via Si^+ or Ge^+ followed by B^+ implantation. One of the major problems with the use of just low energy B^+ is the transient enhanced diffusion (TED) that occurs upon post-implantation annealing. During TED the boron tail region moves significantly and boron diffusivity may be thousands of times greater than the intrinsic value. This enhancement is transient in nature because it stops within a relatively short time, e.g., tens of seconds at 900 °C.[2]

Significant effort has been spent trying to understand and model TED.[3–7] TED is known to arise from implantation induced damage which evolves into a supersaturation of interstitials subsequent annealing. These excess interstitials can enhance the boron diffusivity through interstitial or interstitialcy mechanisms; thus understanding the evolution of these excess interstitials is critical to modeling of TED. The excess interstitials that are not bound to dopants are initially trapped in small clusters[8] and subsequently grow into extended defects, including dopant clusters,[9] {311} defects,[10] dislocation loops,[11] etc.

Recently, Eaglesham *et al.*[10] and Stolk *et al.*[12] have shown that for a 40 keV, $5\times10^{13}/cm^2$ Si implant the excess interstitials driving TED originate from the dissolution of {311} defects upon annealing. The time and temperature of TED coincided with the {311} defect dissolution process leading them to conclude that {311}'s were the source of the TED. Cowern *et al.*[13] have also claimed that for a relatively high implant dose (⩾$10^{13}/cm^2$ for 50 keV Si), TED can be attributed to interstitials emitted from {311} defects. However, these results were for self implants into undoped regions. Zhang *et al.*[9] have reported TED occurs in samples implanted with 4 keV, $1\times10^{14}/cm^2$ boron where no {311} or any other extended defects were observed. Their results implied that there may be more than one source of interstitials for TED when dopants are in the implanted region.

The purpose of this work was to study TED from B+ implants alone as a function of implant energy. Transmission electron microscopy (TEM) is used to determine the microstructure upon annealing. By increasing the energy, it is shown that one can go from a region of no {311} defects to a region of high concentration of {311} defects for the same dose. The interstitial release from the implanted region was studied by measuring the enhancement in the diffusion of boron in δ-doping superlattices.[14] By comparing the defect and diffusion behavior, it is shown that formation of {311} defects dramatically increases the duration of TED.

[a)]Electronic mail: kjones@eng.ufl.edu

Downloaded¬25¬Mar¬2011¬to¬128.227.207.19.¬Redistribution¬subject¬to¬AIP¬license¬or¬copyright;¬see¬http://jap.aip.org/about/rights_and_permissions

II. EXPERIMENT

Boron δ-doping superlattices were grown by low temperature molecular beam epitaxy (LTMBE) on float zone Si(100) substrate with boron doped to a resistivity of 1000 Ω cm.[15] The samples contain six 100-Å-wide box shaped boron spikes with a separation of about 1000 Å and a peak concentration of about $1.4\times10^{18}/\mathrm{cm}^3$. This low concentration keeps boron diffusion intrinsic for the as-grown control samples during the following anneals and avoids the complication of extrinsic effects. Boron ions were implanted into the superlattices at energies of 5, 10, 20, and 40 keV to a dose of $2\times10^{14}/\mathrm{cm}^2$ at a current of 0.1 mA and at room temperature. The samples were then annealed at 750 °C for times of 3 min, 15 min, and 2 h in a nitrogen ambient. The temperature error range is estimated to be ±10 °C. Due to the finite rise time of the sample temperature, the error range for the 3 min sample could be ±30 °C. The initial boron profile as well as the profiles after implantation and annealing were measured by secondary ion mass spectroscopy (SIMS) with 3.0 keV O_2^+ at a current of 50 nA. The raster size was 150×150 $\mu\mathrm{m}^2$ and the analyzed area was 60×60 $\mu\mathrm{m}^2$. The broadening of profiles was simulated using the process simulator PROPHET.[16] The spikes merged into the implant damage region were excluded from the simulation. Plan-view TEM (PTEM) samples were prepared from the annealed superlattices using the standard jet etching procedure using HF:HNO_3 solution. TEM micrographs were taken under weak beam dark field conditions using a JEOL 200CX microscope.

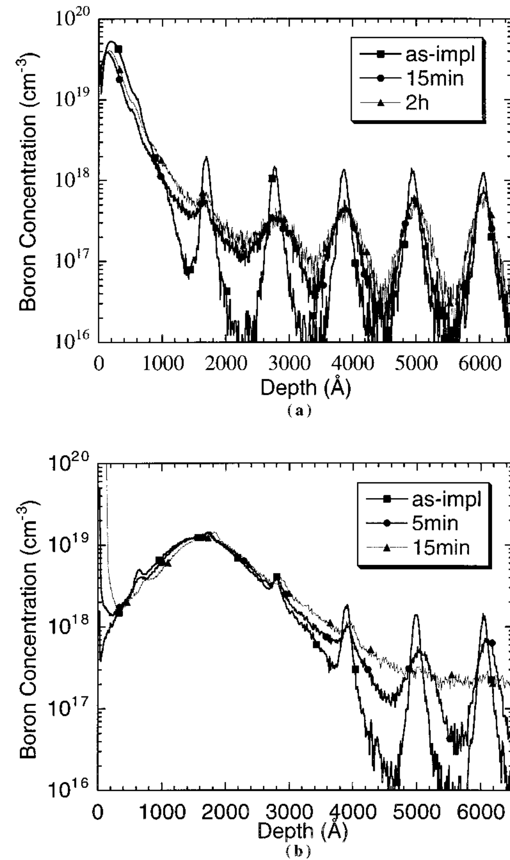

FIG. 1. SIMS profiles of (a) 5 keV and (b) 40 keV B^+ implanted superlattices at a dose of $2\times10^{14}/\mathrm{cm}^2$, as implanted and annealed at 750 °C for 3 min, 15 min, and 2 h in N_2.

III. RESULTS AND DISCUSSION

SIMS profiles of boron in the superlattices are selectively shown in Fig. 1. Figure 1(a) shows the profiles after 5 keV B^+ implantation and annealing, while Fig. 1(b) shows the profiles after 40 keV B^+ implantation and annealing. As can be seen, the higher energy results in a deeper implant profile and a greater enhanced diffusion of the buried boron spikes. The time-averaged boron diffusivities for a particular spike, $\langle D_B\rangle$, were extracted by finding the value of D_B in the simulation that resulted in the best match between diffused and target profiles. Using the literature value of $D_B^*=0.757\exp(-3.46/kT)$,[17] the diffusivity enhancement $\langle D_B\rangle/D_B^*$ from the implants was estimated. For the inert ambient annealed control samples, it is expected that no diffusion enhancement occurs, i.e., $\langle D_B\rangle/D_B^*=1$ or $\langle D_B\rangle=D_B^*$. In order to test this, an un-implanted DSL sample was annealed in an inert ambient for 2 h at 750 °C. The estimation of $\langle D_B\rangle$ was done via matching of the SIMS and the simulation. Taking an average over the six different spikes, since $\langle D_B\rangle$ is depth independent, $\langle D_B\rangle$ is found to be 1.6×10^{-17} $\mathrm{cm}^2/\mathrm{s}\pm0.7\times10^{-17}$ cm^2/s or about two times greater than the predicted value of 7.2×10^{-18} cm^2/s. This is within the error range of furnace and SIMS analysis accuracy and our knowledge of D_B^*.

Figures 2(a)–2(d) are plots of $\langle D_B\rangle/D_B^*$ as a function of depth for different implant energies after each anneal. The program assumes that the total sheet concentration is preserved for each spike during diffusion, i.e., the depth integration of boron concentration under each spike remains a constant after implantation and annealing. However, the influx from the surface implant into the spike region violates the conservation. The error bars of $\langle D_B\rangle/D_B^*$ shown do not include this effect. The dots in Fig. 2 are the data points and the lines are exponential fitting curves. We can see that the value of $\langle D_B\rangle/D_B^*$ decays exponentially with increasing depth, and the decay length is smaller at a shorter annealing time (3 min) than longer times (15 min and 2 h). The cross of $\langle D_B\rangle/D_B^*$ curves for the 3 and 15 min anneals implies that the interstitials have not diffused deep enough to cause a large diffusion enhancement after a short time. The slightly positive slopes of the $\langle D_B\rangle/D_B^*$ curves for the 15 min and 2 h anneals in the 40 keV implant are not significant and might be due to SIMS analysis and/or simulation error. After a short time anneal, for each particular spike, the value of $\langle D_B\rangle/D_B^*$ increases with increase of implant energy. For example, for a boron spike at a depth of around 3800 Å, after an anneal of 3 min, the 5 keV implant shows an enhancement of about 260, whereas the 40 keV implant shows a much greater enhancement of about 2800. As the anneal time increases, this difference is less distinguishable for energies above 5 keV.

Boron atoms diffuse mostly via an interstitial/interstitialcy mechanism. The diffusivity enhancement $\langle D_B\rangle/D_B^*$ is therefore proportional to the time-averaged supersaturation of silicon self-interstitials $\langle C_I\rangle/C_I^*$ given by

Downloaded¬25¬Mar¬2011¬to¬128.227.207.19.¬Redistribution¬subject¬to¬AIP¬license¬or¬copyright;¬see¬http://jap.aip.org/about/rights_and_permissions

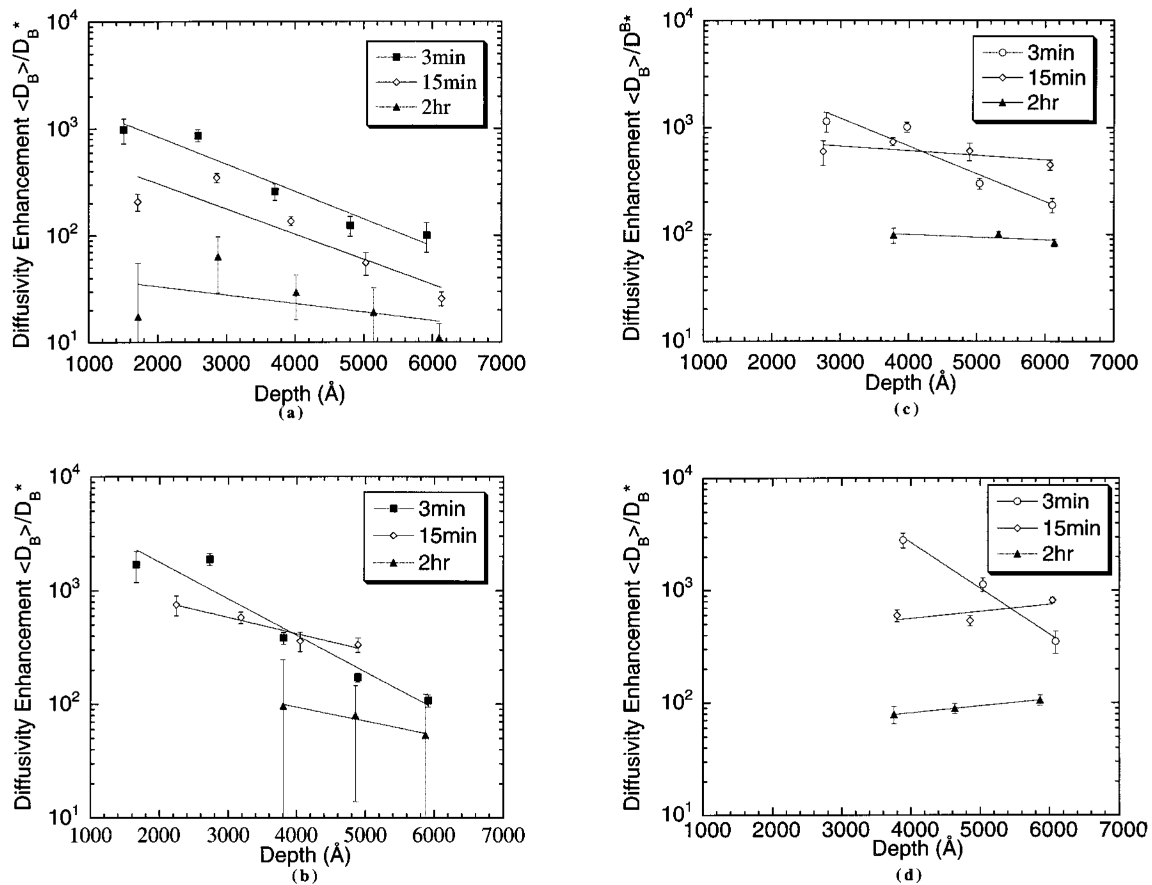

FIG. 2. Enhancement of boron diffusivity after B^+ implantation at an energy of (a) 5 keV, (b) 10 keV, (c) 20 keV, and (d) 40 keV to a dose of $2\times10^{14}/cm^2$, annealed at 750 °C for 3 min, 15 min, and 2 h in N_2.

$$\frac{\langle D_B\rangle}{D_B^*}=\frac{\langle C_I\rangle}{C_I^*}=\frac{1}{t}\int_0^t\frac{C_I}{C_I^*}dt_1, \qquad (1)$$

where C_I is the instantaneous self-interstitial concentration at time t_1 and t is the diffusion time. If we assume that the excess interstitials introduced by an implant are trapped in interstitial-containing defects in the initial stage of the annealing, then we can consider these defects as an interstitial reservoir that keeps C_I/C_I^* constant for a short period of time ($t<t_0$). If at time $t>t_0$ all the interstitial-containing defects have dissolved, then the reservoir is empty and C_I/C_I^* drops abruptly to 1. This process can be expressed as

$$\frac{C_I}{C_I^*}=\begin{matrix}1+E & (t<t_0)\\ 1 & (t>t_0)\end{matrix}, \qquad (2)$$

where E is the supersaturation of interstitials. The integral of Eq. (2) would then become

$$\frac{\langle D_B\rangle}{D_B^*}=\begin{matrix}\frac{1}{t}\int_0^t(1+E)dt_1=1+E & (t<t_0)\\ \frac{1}{t}\left[\int_0^{t_0}(1+E)dt_1+\int_{t_0}^{t}dt\right]=1+\frac{t_0}{t}E & (t\geqslant t_0)\end{matrix}. \qquad (3)$$

From the above equation we can see that $\langle D_B\rangle/D_B^*-1$ is a constant as a function of time for $t<t_0$ and drops approximately as $1/t$ for $t\geqslant t_0$. The breaking point t_0 is the time when the interstitial concentration reaches equilibrium value and TED is completed. This is of course a simplified scenario since TED sources do not turn off abruptly, but rather the interstitial supersaturation decays smoothly over the time period studied. Figure 3 shows a plot of $\langle D_B\rangle/D_B^*-1$ versus annealing time for different implant energies. Because of the finite speed of interstitial diffusion, we have to choose a fixed distance from the interstitial source to make the comparison. A distance of 3600 Å from the projected range of each implant was thus chosen in this plot. Because of the

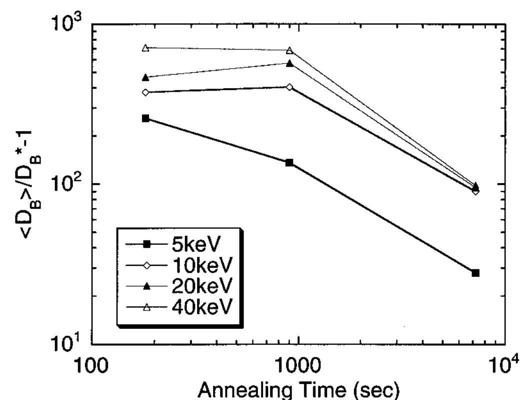

FIG. 3. $\langle D_B\rangle/D_B^*-1$ at a distance of 3600 Å from the projected range as a function of annealing time for different implant energies.

Downloaded¬25¬Mar¬2011¬to¬128.227.207.19.¬Redistribution¬subject¬to¬AIP¬license¬or¬copyright;¬see¬http://jap.aip.org/about/rights_and_permissions

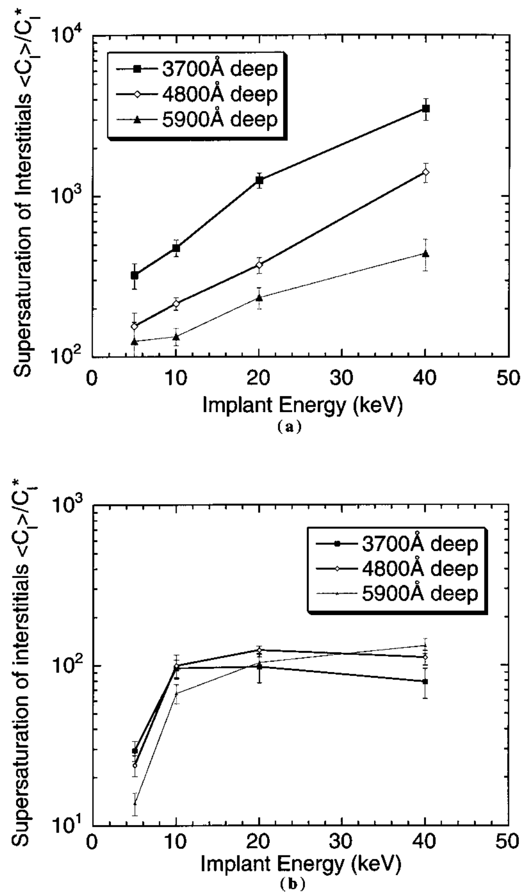

FIG. 4. Supersaturation of interstitials as a function of implant energy after annealing at 750 °C for (a) 3 min and (b) 2 h.

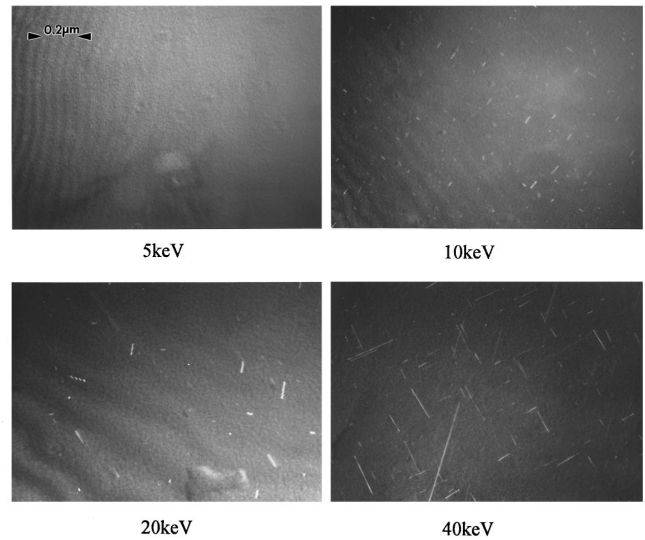

FIG. 5. Plan-view TEM weak beam dark field images ($\mathbf{g}_{220}$) of 5, 10, 20, and 40 keV B^+ implanted into doping superlattices to a dose of $2\times10^{14}/cm^2$ and annealed at 750 °C for 15 min in N_2.

limited number of data points we see just one breaking point t_0 for $E>5$ keV. According to the above discussion, TED is completed before 15 min for the 5 keV implanted and within 15 min–2 h for higher energy implants.

The energy dependence of the time-averaged interstitial supersaturation $\langle C_I\rangle/C_I^*$ after 3 min and 2 h anneals is shown in Fig. 4. For the 3 min anneal the interstitial supersaturation near the implant damage region is much higher than that for larger depth and, as a result, the boron peaks near the implant damage region broaden much more than the deeper boron spikes. As time increases, this difference becomes less marked since the longer time allows for the excess interstitials to diffuse to deeper regions. For the 3 min anneal, the overall trend shows $\langle C_I\rangle/C_I^*$ decreasing with increasing depth and increasing with increasing implant energy. For the 2 h anneal, the depth and energy dependencies of $\langle C_I\rangle/C_I^*$ become much less prominent except for the lowest energy, 5 keV. The reason for the lesser amount and shorter duration of TED at 5 vs 10 keV may be related to several factors, including the source of the interstitials, as will be discussed later.

Figure 5 shows PTEM micrographs of 5, 10, 20, and 40 keV B^+ implanted superlattices after 15 min anneal at 750 °C. There were no defects observed after any of the anneals for the 5 keV implanted samples. The {311} defects were observed in the higher energy implanted samples, with the average defect size increasing with increasing implant energy. The {311} defects dissolve very fast. After 3 min, the defects occur as small clusters and very short rods. After 15 min, the {311} defects coarsen into rods with a reduction in density. After 2 h, the {311} defects dissolve completely in the 10 keV B^+ implanted sample, while in 20 and 40 keV samples, they continue to grow to form longer rods or unfaulted dipoles.

It is important to note that, although there are no {311} defects in the 5 keV B^+ implanted material, TED of boron does occur. For this 5 keV sample annealed at 750 °C, for times of 3 min–2 h, the diffusivity enhancement reduces from 980 to 17 for the second shallowest spike and from 100 to 11 for the deepest one. Because of the relative proximity of the implant damage to the surface at this low energy, a large part of the interstitials could be attracted to the surface so that the supersaturation of remaining interstitials is not sufficient to form extended defects. In addition, the increase in boron peak concentration with decreasing implant energy can lead to the increase in the formation of B-B pairs which form the clustered fraction of the as-implanted profile. These clusters are believed to decrease the number of interstitials that form by reducing the number of boron atoms that move onto substitutional sites.[18] The results of Haynes *et al.*[18] suggest that boron concentrations above $1\times10^{19}/cm^2$ are sufficient to prevent ⟨311⟩ formation from a Si^+ implant. All of these B implants had some fraction of their implant profile above this concentration and the bulk of the profiles showed no motion consistent with clustering. Thus it is possible that increased surface interaction and increased clustering are both contributing to the lack of ⟨311⟩ formation. Despite the fact that ⟨311⟩ defects do not form, excess interstitials still exist and can diffuse into the bulk resulting in enhanced dopant diffusion. Zhang *et al.*[9] have previously reported that TED was observed in 4 keV $1\times10^{14}/cm^2$ B^+ implanted Si without the existence of {311} defects. They attribute the source of interstitials driving TED to submicroscopic clus-

Downloaded¬25¬Mar¬2011¬to¬128.227.207.19.¬Redistribution¬subject¬to¬AIP¬license¬or¬copyright;¬see¬http://jap.aip.org/about/rights_and_permissions

ters, i.e., mobile boron interstitial complexes, which break up during annealing and provide interstitials for TED. They determined the duration of TED by noting when TED stops within the bounds of the SIMS resolution, and their TED saturation was 3–13 min at 750 °C, much shorter than others have reported for TED saturation with {311} defects. These values are very consistent with the TED saturation time discussed in Fig. 3 for the 5 keV B^+ implant. It is possible that the TED observed for the 5 keV sample arises simply from the formation of boron implant B-I pairs[19,20] immediately after implantation and the duration for TED is simply the time necessary for these defects to break up and the excess interstitials to recombine either in the bulk or at the surface. However, it is proposed that when {311} defects exist, because their dissolution process provides interstitials for the formation of mobile boron-interstitial complexes, TED continues for much longer periods of time. Thus as implant energies decrease, the dominant mechanisms controlling the duration of the TED process also change from one controlled by ⟨311⟩ defects to one controlled by nonvisible B-I complexes.

IV. CONCLUSIONS

In summary, boron δ-doping superlattices have been used to study the effect of implant energy on TED in B^+ implanted samples. Higher implant energy (>5 keV) causes more total diffusion enhancement and longer transient diffusion time. For implant energies $\geqslant$10 keV, ⟨311⟩ defects are observed in the microstructure and their concentration increased with implant energy. The 5 keV implant showed no {311} defects after annealing but did show boron TED. A critical distance between the damage region and the sample free surface is believed to exist, below which surface recombination plays an important role in reducing the total number of interstitials in the bulk sufficiently to prevent formation of ⟨311⟩ defects. When ⟨311⟩ defects do form, the duration of TED is dramatically increased.

ACKNOWLEDGMENTS

The authors wish to thank C. S. Rafferty for providing the use of his process simulator PROPHET. The work performed at UF was supported by a contract with SEMATECH.

[1] S. N. Hong, G. A. Ruggles, J. J. Wortman, E. R. Myers, and J. J. Hren, IEEE Trans. Electron Devices **38**, 28 (1991).
[2] P. Packan, Ph.D. dissertation, Stanford University, 1991.
[3] R. T. Hodgson, V. R. Deline, S. Mader, and J. C. Gelpey, Appl. Phys. Lett. **44**, 589 (1984).
[4] A. E. Michel, W. Rausch, P. A. Ronsheim, and R. H. Kastl, Appl. Phys. Lett. **50**, 416 (1987).
[5] T. O. Sedgwick, A. E. Michel, V. R. Deline, S. A. Cohen, and J. B. Lasky, J. Appl. Phys. **63**, 1452 (1988).
[6] Q. Guo, X. Bao, J. Hong, Y. Yan, and D. Feng, Appl. Phys. Lett. **54**, 1433 (1989).
[7] P. A. Packan and J. D. Plummer, Appl. Phys. Lett. **56**, 1787 (1991).
[8] F. Cembali, M. Sorvidori, E. Landi, and S. Solmi, Phys. Status Solidi A **94**, 315 (1986).
[9] L. H. Zhang, K. S. Jones, P. H. Chi, and D. S. Simons, Appl. Phys. Lett. **67**, 2025 (1995).
[10] D. J. Eaglesham, P. A. Stolk, H.-J. Gossmann, and J. M. Poate, Appl. Phys. Lett. **65**, 2305 (1994).
[11] K. S. Jones, S. Prussin, and E. R. Weber, Appl. Phys. Lett. **45**, 1 (1988).
[12] D. J. Eaglesham, P. A. Stolk, H.-J. Gossman, T. E. Haynes, and J. M. Poate, Nucl. Instrum. Methods Phys. Res. B **106**, 191 (1995).
[13] N. E. B. Cowern, G. F. A. van de Walle, P. C. Zaim, and D. W. E. Vandenhoudt, Appl. Phys. Lett. **65**, 2981 (1994).
[14] H.-J. Gossmann, C. S. Rafferty, H. S. Luftman, F. C. Unterwald, T. Boone, and J. M. Poate, Appl. Phys. Lett. **63**, 639 (1993).
[15] H.-J. Gossmann, F. C. Unterwald, and H. S. Luftman, J. Appl. Phys. **73**, 8237 (1993).
[16] M. R. Pinto, D. M. Boulin, C. S. Rafferty, R. K. Smith, W. M. Coughran, Jr., I. C. Kizilyalli, and M. J. Thoma, Proc. IEDM **92**, 923 (1992).
[17] R. B. Fair, in *Impurity Doping Process in Silicon*, edited by F. F. Yang (North-Holland, Amsterdam, 1981), p. 315.
[18] T. E. Haynes, D. J. Eaglesham, P. A. Stolk, H.-J. Gossman, D. C. Jacobson, and J. M. Poate, Appl. Phys. Lett. **69**, 1376 (1996).
[19] N. E. B. Cowern, H. F. F. Jos, and K. T. F. Jannssen, J. Appl. Phys. **68**, 6191 (1990).
[20] N. E. B. Cowern, A. Cacciato, J. S. Custer, F. W. Saris, and W. Vandervorst, Appl. Phys. Lett. **68**, 1150 (1996).

Downloaded¬25¬Mar¬2011¬to¬128.227.207.19.¬Redistribution¬subject¬to¬AIP¬license¬or¬copyright;¬see¬http://jap.aip.org/about/rights_and_permissions